Chapter 7

Phase Transitions and Physical Properties of a Binary Mixture of Bicyclohexane Compounds: Refractive Index and X-ray Diffraction Measurements

7.1 Introduction:

Liquid crystal material research have contributed significantly both to the development of liquid crystal display (LCD) technology and also at the same time to the better understanding of the phase behaviour of soft condensed matter systems. Thus, attempts are being continuously made to study the material properties of both pure compounds as well as their mixtures for a better insight into the basic understanding of liquid crystalline behaviour, so that better display devices can be made.

In this chapter, I present the phase diagram, DSC, birefringence, density and x-ray diffraction measurements of a binary mixture of two isomeric non-polar bicyclohexane compounds containing alkenyl side chains. So far, there are only a few liquid crystal classes described in the literature whose core consists of two cyclohexane rings. The physical properties of the pure components have been studied previously in our laboratory [1-4]. These two compounds, one comprising of only nematic phase ($1d(3)CCO_2$) and the other only smectic B phase ($0d(4)CCO_2$), are characterized by similar molecular structure, except for a shift in the position of the double bond. It has been shown by Schadt et al [5] that, the introduction of a double bond at specific side chain positions markedly affects the physical properties of liquid crystals. With a view to study the effect of the position of double bond in the alkenyl side chain on the mesomorphic properties, mixtures of these compounds have been prepared. Physical properties of these mixtures have been studied at seven different compositions. Phase diagram for this system shows the presence of mixtures with only smectic B phase, only nematic phase and mixtures with both smectic B and nematic phases. A two phase (smectic B - nematic) co-existing region (~2-3°C) has also been observed for

a small concentration range for these mixtures. Differential scanning calorimetric studies on these mixtures have been done and the entropy changes associated with the smectic B - nematic and nematic - isotropic phase transition have been calculated. Densities and refractive indices (n_o, n_e) have been measured for these mixtures. The refractive index data have been analyzed to yield orientational order parameters. From the DSC, density and birefringence measurements, the nature of the smectic B - nematic phase transition for these mixtures and the behaviour of these phase transitions with concentration has been assessed.

For x-ray diffraction measurements we have selected a few compositions of this mixture, which show both the smectic B and nematic phases. Two mixtures with molar concentration of 1d(3)CCO$_2$ = 0.6 (Mixture A) and 0.73 (Mixture B) have been studied thoroughly throughout the entire mesomorphic range. DSC studies for these two mixtures show a weakly first order or a second order phase transition in going from the smectic B to the nematic phase.

According to Birgeneau and Lister [6], the smectic B phase is a realization of the stacked hexagonal phase possessing BOO found in two dimensions. The order parameter associated with a system having six-fold symmetry, as in the case of smectic B liquid crystals is the Bond Orientational Order, defined to be the thermal average of the quantity

$$\psi(r) = \langle \exp (i6\theta(r)) \rangle \qquad \textbf{7.1}$$

where, the bond angle $\theta(\mathbf{r})$ is the orientation, relative to any fixed laboratory axis, of a bond between two nearest neighbour molecules. The x-ray

diffraction patterns have been analysed to determine the temperature dependence of the Bond Orientational Order (BOO) in the smectic B phase of only mixture A, where it has been possible to obtain a good mono-domain sample.

Orientational order parameters have also been studied throughout the entire mesomorphic range for mixtures A and B. The intermolecular distance, layer thickness and apparent molecular lengths of several mixtures (x = 0.3, 0.4, 0.5, 0.6 and 0.73, where x is the mole fraction of 1d(3)CCO_2)) have also been studied. Although x-ray [7-13] and electron diffraction [14,15] studies on smectic B phase have been reported so far, not much work has been done to determine the BOO and OOP in smectic B phase of bicyclohexane compounds. The BOO values obtained have been utilized to characterize the SmB phase which is found to be of the crystal B type. The BOO values of mixture A are found to be nearly independent of temperature in the SmB phase but increases with temperature within the co-existing SmB-N phase. The transverse correlation length diverges near the vicinity of the two-phase co-existing SmB-N region indicating a second order phase transition.

7.2 Experimental:

Phase diagram and texture study:

The compounds were donated by M/S Hoffmann-La-Roche and Co., Basel, Switzerland and were used without further purification. Phase transitions of the pure samples as well as their mixtures were studied by observing textures under crossed polariser with a polarizing microscope equipped with

a Mettler FP80/82 Thermo-system. The structural formula, transition temperatures and chemical name of the pure compounds are as follows:

Compound 1:

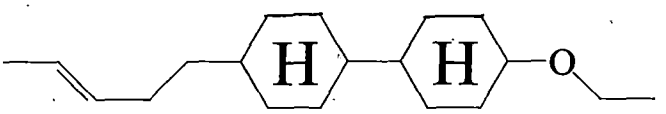

$$K \underset{24.5^{\circ}C}{\overset{44^{\circ}C}{\rightleftharpoons}} N \xrightarrow{76.5^{\circ}C} I$$

4(3″- pentenyl) 4′(ethoxyl) 1,1′ bicyclohexane (1d(3)CCO_2)

Compound 2:

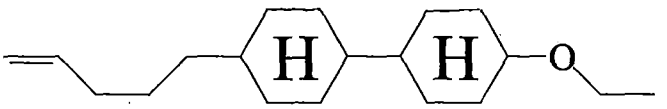

$$K \xrightarrow{11^{\circ}C} Sm\ B \xrightarrow{43^{\circ}C} I$$

4-ethoxy, 4′ - pent - 4″- enyl bicyclohexane (0d(4)CCO_2)

The phase diagram of this system is shown in figure 6.1. The nematic-isotropic and smectic B-nematic transition temperatures are plotted against mole-fraction (x) of 1d(3)CCO_2 in figure 6.1. It has only been possible to measure the supercooling temperature for mixture with x = 0.71 and the pure compound 1d(3)CCO_2 due to lack of cooling facilities in our laboratory. Texture study of these mixtures showed typical marbled texture in the nematic phase and a mosaic texture in smectic B phase.

DSC measurements:

Transition entropies ΔS (J $mol^{-1}K^{-1}$) were obtained from DSC studies (at a heating rate of 1°C/min) using a Mettler FP84HT TA Cell.

Density measurements:

The densities of all the binary mixtures were measured with the help of dilatometer of the capillary type. Density measurement of the pure compounds has already been done in our laboratory [1-2]. Temperature during the experiment is controlled to about ± 0.5°C by a temperature controller. Experimental uncertainty of the density measurement is 0.1%.

Refractive Index measurements:

The ordinary and extraordinary refractive indices (n_o, ne) for wavelength λ = 5780Å of mercury vapour lamp were measured within ± 0.001 by thin prism method (refracting angle < 2°) [16]. Details of the experimental technique used have been described in chapter-2 of this thesis. From the density and refractive index values, I have calculated the principal polarizabilities ($\alpha_{\|}$,$\alpha_{\perp}$) using Neugebauer's anisotropic internal field model [17] and Haller's extrapolation procedure [18].

X-ray diffraction Measurements:

X-ray diffraction patterns are recorded using a flat plate camera at several temperatures within the mesomorphic phase using Ni filtered CuK_{α} radiation of wavelength λ = 1.542Å. For x-ray diffraction study, the pure compounds as well as their mixtures could not be aligned even in a magnetic field of about 0.6T. The magnetic susceptibility anisotropy, $\Delta\chi$ for these compounds being almost zero, it is not possible to obtain monodomain samples by application of magnetic field. However, I succeeded in obtaining very good

monodomain samples in which the hexagonal symmetry of the SmB phase extended throughout the bulk sample by controlled cooling (at the rate of 0.1°C/min) of the samples kept in 0.5mm diameter glass capillaries, from the isotropic state to room temperature (~20°C). By trial a monodomain sample was selected and the capillary is rotated in such a way that the layer normal coincided with the direction of the x-ray beam. At this position of the capillary x-ray photographs are recorded. Photographs for orientational order parameter measurements are taken after rotating the sample filled capillary 90 degrees with respect to the previous position such that the smectic layer is now parallel to the direction of x-ray beam.

The x-ray diffraction photographs are scanned by a Mustek 1200 UB scanner. The gray mode scan is used and the resolution was set at 600 dpi. Optical densities of the pixels are calculated and then converted to X-ray intensities with the help of a calibration curve following the procedure of Klug and Alexander [19]. The Origin 7.0 software is used for data analysis purpose.

7.3 Results And Discussions:

From a detailed study of the phase diagram by microscopic observations, it is observed that for mixtures within the concentration range $0.2 < x < 0.8$ (x = mole fraction of 1d(3)CCO2), both smectic B and nematic phases are present. Mixtures with $x < 0.2$ show smectic B phase only and for $x > 0.8$ show only nematic phase.

For mixtures with mole fraction between x ≈ 0.5 to x ≈ 0.8 a two-phase (SmB- N) co-existing region of 2-3°C is observed. The phases could be identified distinctly under polarizing microscope and the co-existing phases are quite stable. All the mixtures show large super cooling.

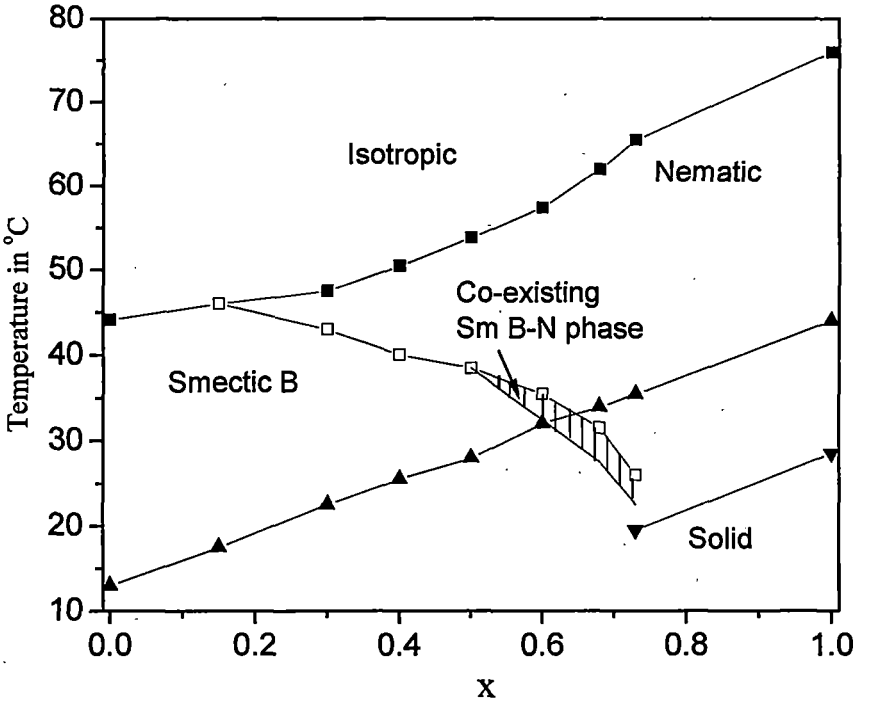

FIGURE 7.1: Phase diagram for the binary system of 1d(3)CCO_2 and 0d(4)CCO_2 . x is the mole fraction of 1d(3)CCO_2. ■ nematic (smectic B) - isotropic transition temperature. □ smectic B- nematic transition temperature; ▲ melting temperature; ▼ super- cooling transition temperature; shaded region represent the co-existing smectic B - nematic phase.

The isotropic transition temperature for these mixtures lie significantly below the straight line connecting those of the pure compounds and a fairly deep minimum is observed in the clearing curves for x ≈ 0.4. The melting temperatures for these mixtures however follow the additive rule.

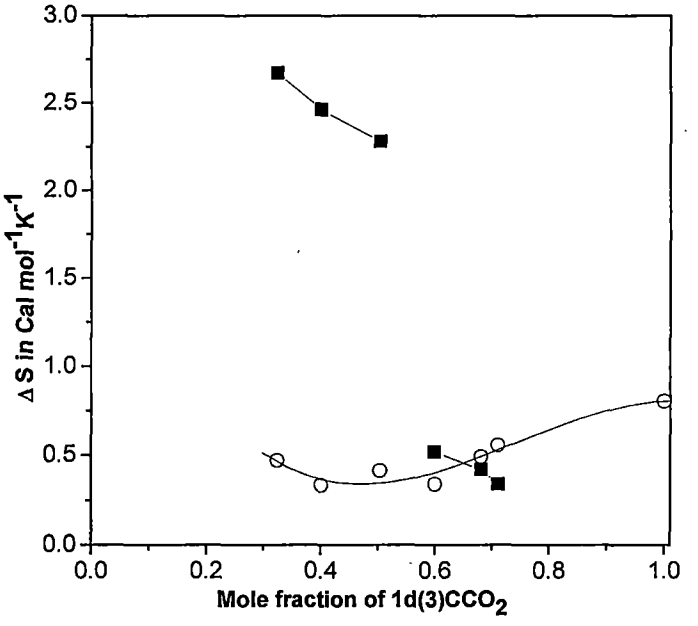

FIGURE 7.2: Transition entropies (ΔS) as a function of mole fraction of 1d(3)CCO_2 : ■ smectic B/nematic transition, ○ nematic/isotropic transition.

Figure 7.2 shows the entropy change associated with the smectic B - nematic and nematic - isotropic phase transition plotted against mole fraction of 1d(3)CCO_2. From the figure it is evident that the entropy change associated with the smectic B - nematic phase transition for these mixtures decreases linearly in the region x = 0 to x = 0.55 and then falls rapidly at x = 0.6. This clearly implies a change in the order of this phase transition from discontinuous to continuous at this value of x (= 0.6). The nematic-isotropic entropy change shows a minimum near equimolar concentration.

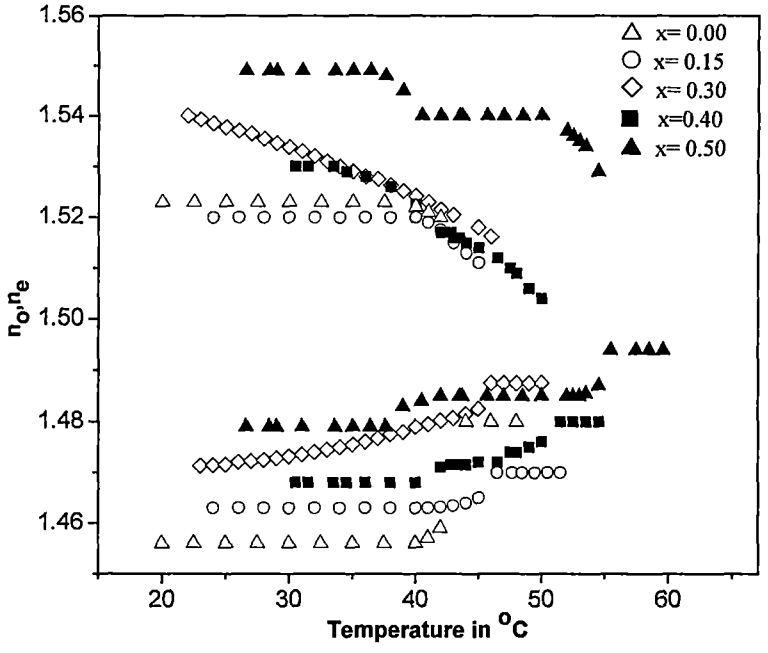

FIGURE 7.3 (a): Refractive indices as a function of temperature for mole-fractions (x) of 1d(3)CCO$_2$. △ (x= 0.0); ○ (x= 0.15); ◇ (x= 0.3); ■ (x= 0.4); ▲ (0.5).

The variation of ordinary (n_o) and extraordinary (n_e) refractive indices with temperature are shown in figures 7.3(a) – 7.3(b) for λ = 5780Å. The ordinary as well as the extraordinary refractive indices are found to be nearly independent of temperature in the smectic B phase, except very near to the smectic B-nematic (or isotropic) transition temperatures for all the mixtures. The n_e and n_o values are however quite sensitive to temperature in the nematic phase. In the co-existing smectic B - nematic phase, I have been able to measure simultaneously the refractive indices of both the smectic B and the nematic phases. The ordinary refractive indices for smectic B and nematic phases are the same, whereas the extraordinary refractive index for the nematic phase (n_{en}) and smectic B phases (n_{es}) are different. The

temperature dependence of n_{es} is large, but n_{en} is more or less independent of temperature.

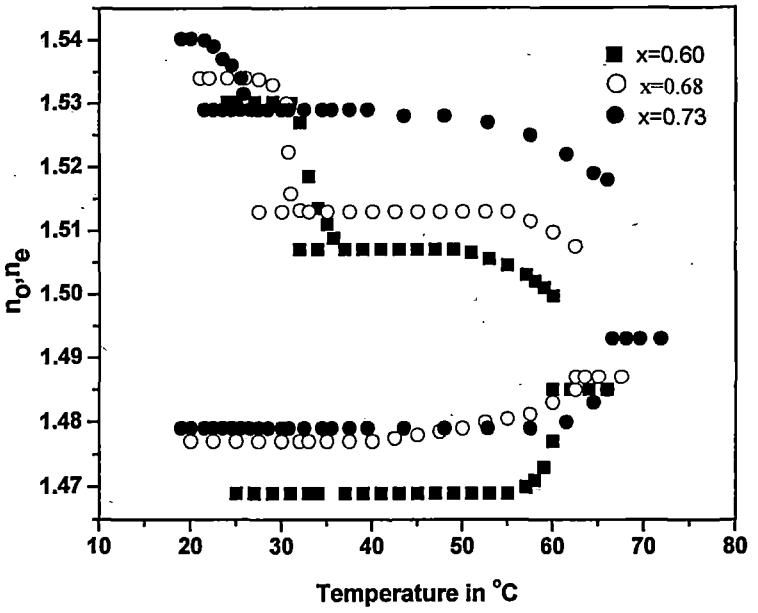

FIGURE 7.3 (b): Refractive indices (n_o, n_e) as function of temperature for different mixtures. ■ x=0.6; ○ x=0.68 ; ● x=0.73.

The optical birefringence Δn (= n_e-n_o) are shown in figures 7.4 (a) – 7.4 (b) for these mixtures, which are found to be very low and is less than 0.1 even in the smectic B phase. The temperature dependence of the density values for different mixtures as well as the pure compounds are plotted in figure 7.5. The change of birefringence as well as density values at the smectic B-nematic phase transition seems to be continuous for $x \geq 0.55$ which indicate a weakly first order or second order phase transition.

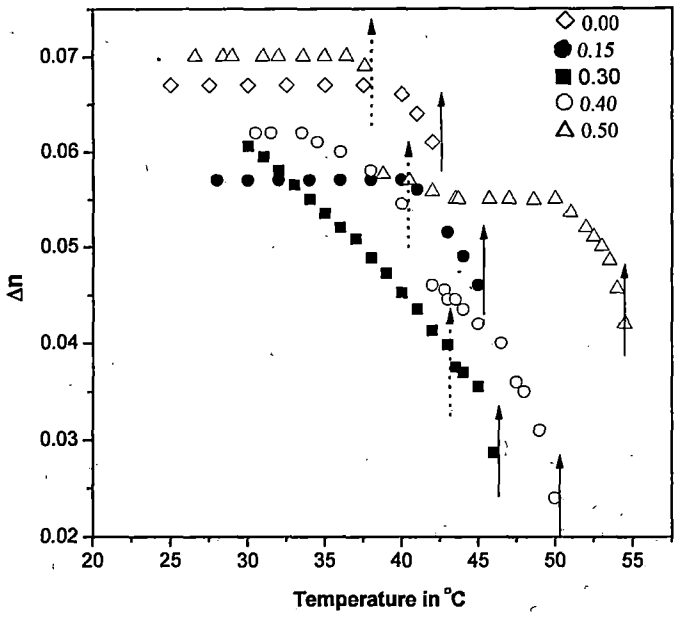

FIGURE 7.4 (a): Birefringence ($\Delta n = n_e - n_o$) as a function of temperature for different mixtures and a pure compound. ◇ (x= 0.0); ● (x= 0.15); ■ (x= 0.30); ○ (x= 0.4); △ (x= 0.5) ; ↑ for nematic to isotropic transition; ↑ for smectic B to nematic transition.

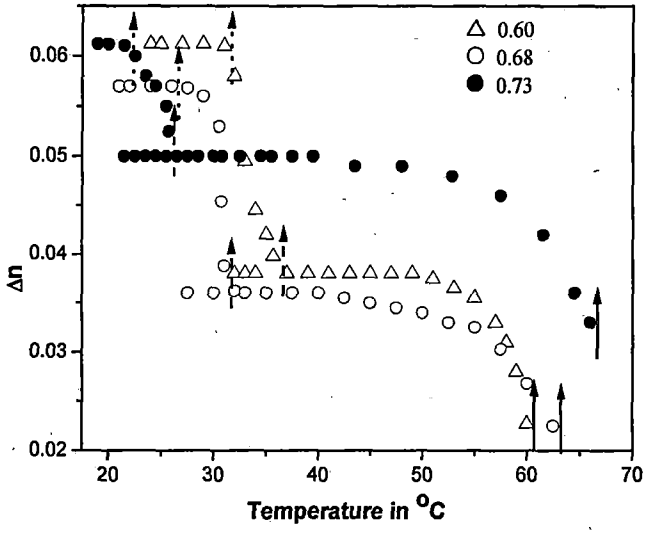

FIGURE 7.4 (b): Birefringence ($\Delta n = n_e - n_o$) as a function of temperature for different mixtures: △ (x= 0.6); ○ (x= 0.68); ● (x= 0.73); ↑ for nematic to isotropic transition; ↑ for coexisting SmB-N to nematic transition; ↑ for SmB to SmB – N coexisting transition.

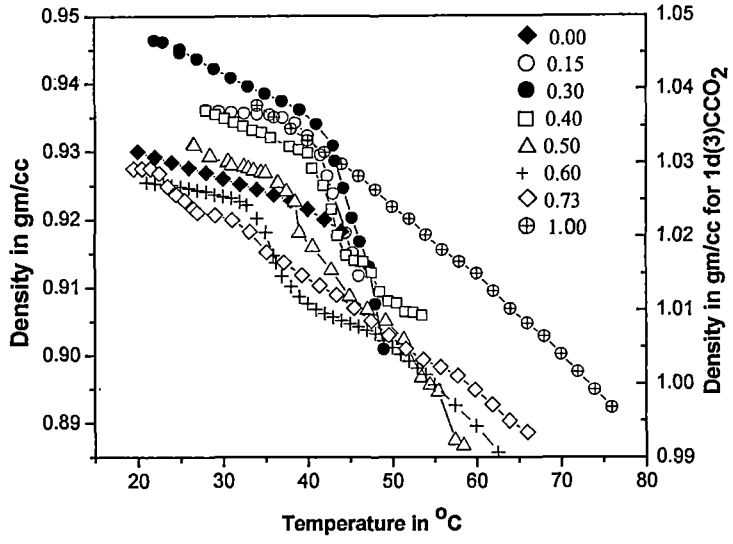

FIGURE 7.5: Density (ρ) values as a function of temperature for different mixtures and pure compounds. ◆ (x= 0.0); ○ (x= 0.15); ● (x= 0.3); □ (x= 0.4); △ (x= 0.5); +(x = 0.6); ◇ (x= 0.73); ⊕ (x= 1.0).

Both birefringence (Δn) and density values changes sharply with temperature within the co-existing smectic B-nematic phase. Also, the temperature dependences of the density values in the smectic B phase are much higher for mixtures with $x \leq 0.55$ than in the smectic B phase for those mixtures with $x \geq 0.55$. Incidentally the two-phase smectic B - nematic co-existence region is present for mixtures with $x \geq 0.55$. The temperature dependences of the density values show a steep variation within the co-existing phase in comparison to its dependence within its nematic and smectic B neighbours. I also observe similar behaviour of birefringence values for these mixtures (figure 7.4).

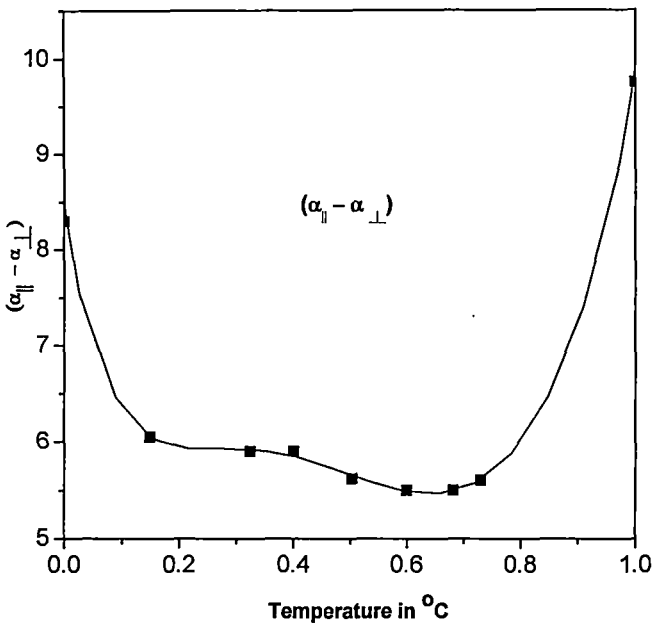

FIGURE 7.6: Variation of $(\alpha_{||} - \alpha_{\perp})$ against mole fraction of 1d(3)CCO_2.
■ Neugebauer's method.

In figure 7.6, I have plotted the polarizability anisotropy ($\Delta\alpha$) values for the pure compounds as well as for the different mixtures. I have observed that a decrease in the values of $\Delta\alpha$ with mole fraction of 1d(3)CCO_2 which shows a broad minimum near $x \approx 0.6$.

The temperature variations of orientational order parameter $\langle P_2 \rangle$ for the different mixtures are shown in figures 7.7(a) – 7.7(b). Similar to the observed trends in the temperature dependences of the density and birefringence, the $\langle P_2 \rangle$ values drops sharply at the nematic – smectic B phase transition for mixtures with $x < 0.5$ once again indicating the order of the nematic-smectic B phase transition for these mixtures to be of first order (figure 7.7(a)).

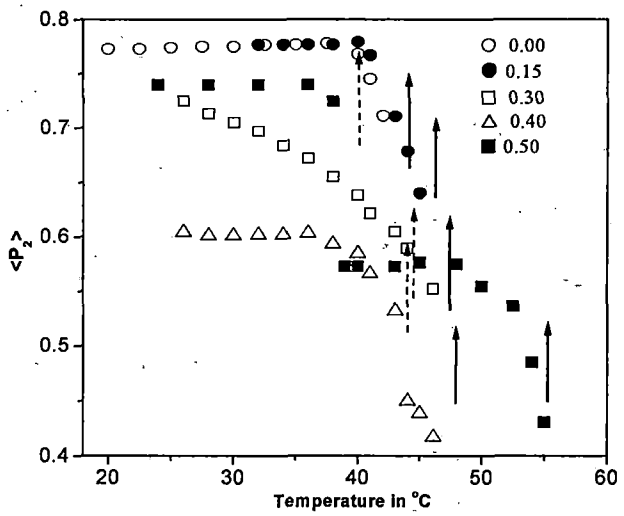

FIGURE 7.7 (a): Orientational order parameter $\langle P_2 \rangle$ as a function of temperature for mole-fractions (x) of ○ 1d(3)CCO_2 (x= 0.0) ; ● (x= 0.15) ; □ (x= 0.3); △ (x= 0.4) ; ■ (x= 0.5) ; ↑ for nematic to isotropic transition; ↑ for smectic B to nematic transition.

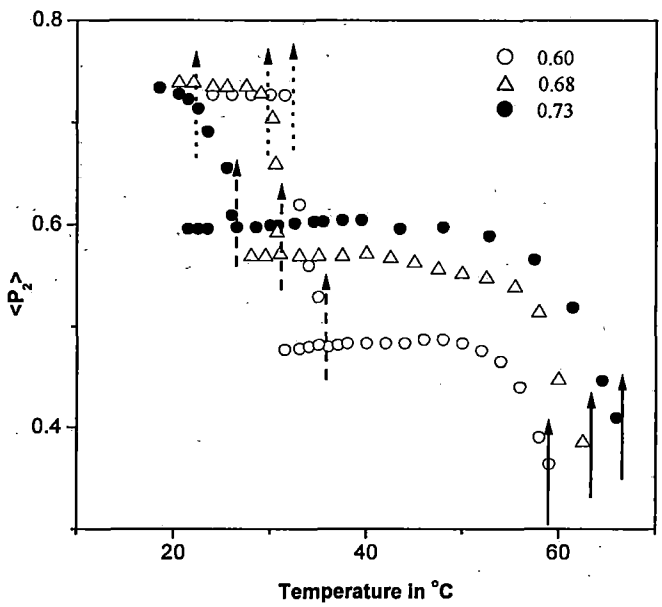

FIGURE 7.7(b): Orientational order parameter $\langle P_2 \rangle$ as a function of temperature for different mixtures with mole-fractions (x) of 1d(3)CCO_2 .○(x= 0.6) ; △ (x= 0.68) ; ● (x= 0.73); ↑ for nematic to isotropic transition ; ↑ for coexisting SmB-N to nematic transition ; ↑ for SmB to SmB – N coexisting transition.

The order parameter values however changes continuously across the nematic – smectic B transition temperatures for mixtures with molar concentration x > 0.5 as indicated in figure 7.7(b). It is also observed that within the co-existing phase the temperature variation of $\langle P_2 \rangle$ is quite sharp which corroborate the results of density and refractive index measurements.

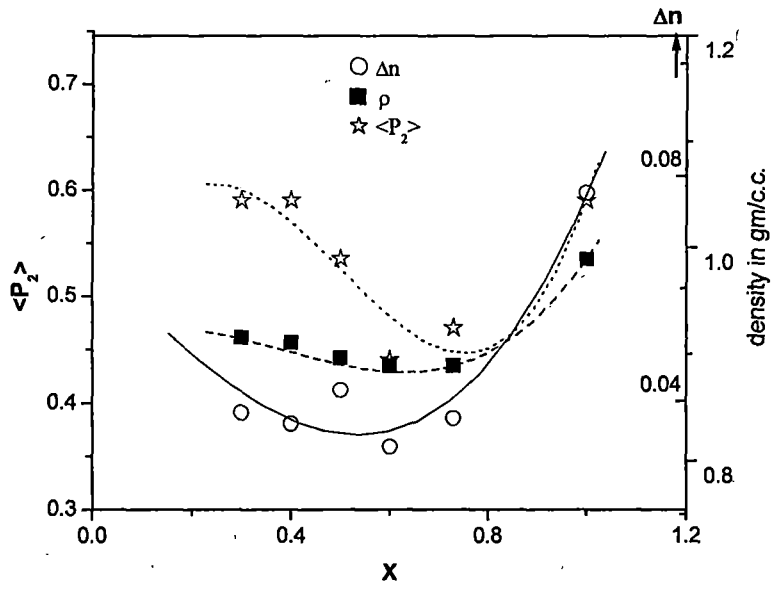

FIGURE 7.8: Density (ρ), $\langle P_2 \rangle$ and Δn against mole fraction of 1d(3)CCO2 at $T = T_{NI}(T_{SI}) - 2\ ^{\circ}C$. (■ ρ, ☆ $\langle P_2 \rangle$, ○ Δn).

Figure 7.8 shows the variation of $\langle P_2 \rangle$, Δn and density with mole fraction of $1d(3)CCO_2$ at a temperature $T = T_{NI}(T_{SI})-2^{\circ}C$. The $\langle P_2 \rangle$, Δn and density values in the nematic phase show a minimum near $x \approx 0.6$.

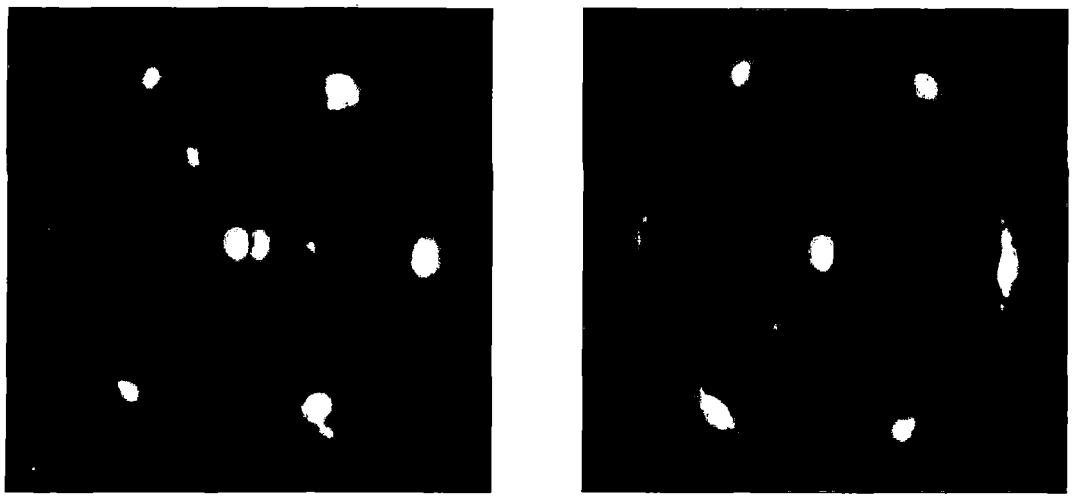

(a) (b)

FIGURE 7.9: X-ray diffraction photograph from an aligned sample of mixture A (x= 0.6001), where the incident x-ray beam parallel to the layer normal. (**a**) Smectic B phase 25°C (**b**) Co-existing SmB-Nematic phase at 35.5° C

Figure 7.9(a) shows the x-ray diffraction photograph of the aligned sample in the smectic B phase of mixture A at 25°C where the incident x-ray beam is parallel to the layer normal. The outer diffraction ring is split up into six spots, clearly showing the hexagonal molecular arrangement within the layers. Almost identical photographs have been observed from room temperature up to the smectic B to nematic phase transition except in the co-existing SmB-N phase. The co-existing phase is marked by the appearance of relatively sharp x-ray diffraction spots exhibiting the hexagonal symmetry of the SmB phase, superimposed on the diffuse liquid like outer ring characteristic of the nematic phase with the direction of the incident beam parallel to the nematic director (figure 7.9(b)), indicating the presence of both nematic and smectic B domains. Similar behaviour of these mixtures has also been observed from refractive index measurements, where I have

been able to observe and measure the refractive indices for both the smectic B and nematic phases in the co-existing region.

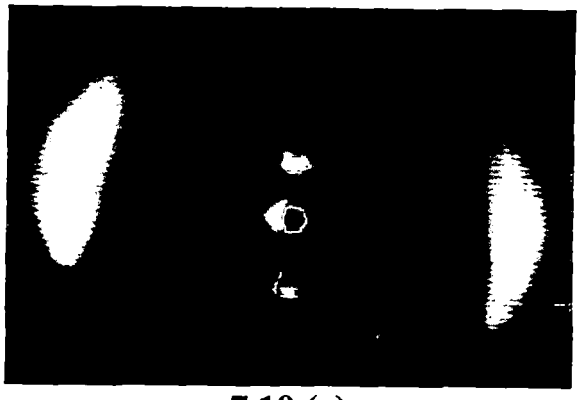

7.10 (a)

7.10(b)

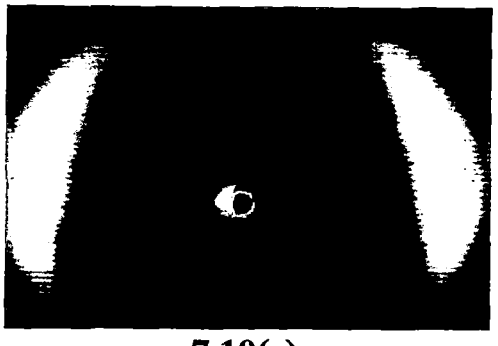

7.10(c)

FIGURE 7.10: X-ray diffraction pattern of an aligned sample of mixture A, where x-ray beam is incident perpendicular to the layer normal: (**a**) x = 0.6 SmB at T = 23°C; (**b**) smectic B-nematic co-existing phase at 35° C; (**c**) nematic phase at 38° C.

The x-ray diffraction pattern of a well oriented monodomain sample of mixture A in the smectic B, smecticB-nematic co-existing phase and nematic phases are shown in figures 7.10(a) - 7.10(c) respectively. These photographs are obtained after slow cooling of a drop of the liquid crystal placed on a glass plate with the x-ray beam incident parallel to the glass plate. The x-ray patterns are recorded using a 2-D area detector (HI – Star, Siemens AG).

The bond orientational order has been calculated by evaluating the expression,

$$\langle \cos(6\theta) \rangle = \int_0^{\pi/6} \cos(6\theta) f(\theta) d\theta \,/\, \int_0^{\pi/6} \cos f(\theta) d\theta \qquad \textbf{7.2}$$

where, f(θ) is the angular distribution function of centre of mass of the neighbouring molecules with respect to a central molecule and the angular distribution function has a maximum at $\theta = 0$. The above equation can be approximated by the following expression,

$$\langle \cos(6\theta) \rangle \approx \int_0^{\pi/6} \cos(6\theta) I(\theta) d\theta \,/\, \int_0^{\pi/6} I(\theta) d\theta \qquad \textbf{7.3}$$

where I(θ) is the azimuthal distribution of the x-ray diffraction intensity. According to Vainshtein [20] it has been assumed that I(θ), the intensity distribution, is proportional to f(θ) the distribution function and consequently has its maximum at $\theta = 0$. BOO is calculated for each peak and finally the average over six peaks are taken. The intensity values plotted against azimuthal angular positions have been corrected for the background (scattered) intensity values.

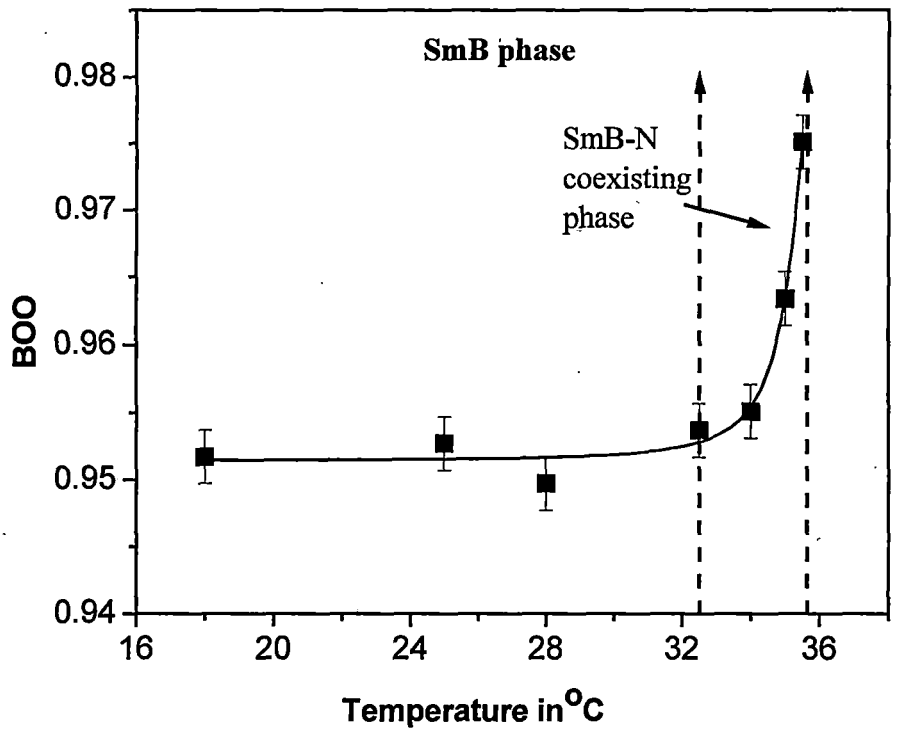

FIGURE 7.11: Temperature variation of bond orientational order (BOO) for mixture A.

Figure 7.11 shows the Bond Orientational Order (BOO) values at different temperatures in the smectic B phase for mixture A. The BOO in the smectic B phase of this mixture is found to be ~ 0.96 and independent of temperature throughout the SmB phase. This result seems to indicate that the smectic B phase for this mixture is of the crystal B type in the sense that the molecular positions exhibit long-range bond orientational order throughout the phase. Interestingly it is found that the BOO values increases rapidly with temperature in the co-existing SmB-N phase. This increase may be due to the pretransitional effect of the SmB-N second order phase transition.

The transverse correlation length in the SmB as well as in the nematic phase of mixtures A and B has been determined from a linear scan of the x-ray diffraction peaks. X-ray intensities are at first corrected for the use of a flat plate camera. This corrected intensity data are then deconvoluted for finite width of the collimator. The deconvoluted intensity profile I(q) is fitted to a Lorentzian form with a quadratic background viz.,

$$I(q) = \frac{a_1}{a_2 + (q - q_o)^2} + a_3 q^2 + a_4 q + a_5 \qquad \textbf{6.4}$$

q being the magnitude of the scattering vector. The transverse correlation length is defined as $\xi = 2\pi(a_2)^{-1/2}$. The in-plane transverse resolution (FWHM) for this instrument is $\Delta q = 6 \times 10^{-3}$ Å^{-1}.The values of the correlation lengths obtained in this way varied from 35Å to 50Å in SmB phase and 18Å to 25Å in nematic phase for these mixtures. For Crystal B phase the correlation lengths are expected to be much longer. One reason for this discrepancy may be due to the use of Ni filtered CuK_α radiation, which contains a white background radiation in addition to the CuK_α peak. No correction for this white radiation, which broadens the diffraction peaks considerably, is made here. Hence the experimental values of correlation lengths as obtained above are much shorter than the theoretically expected values.

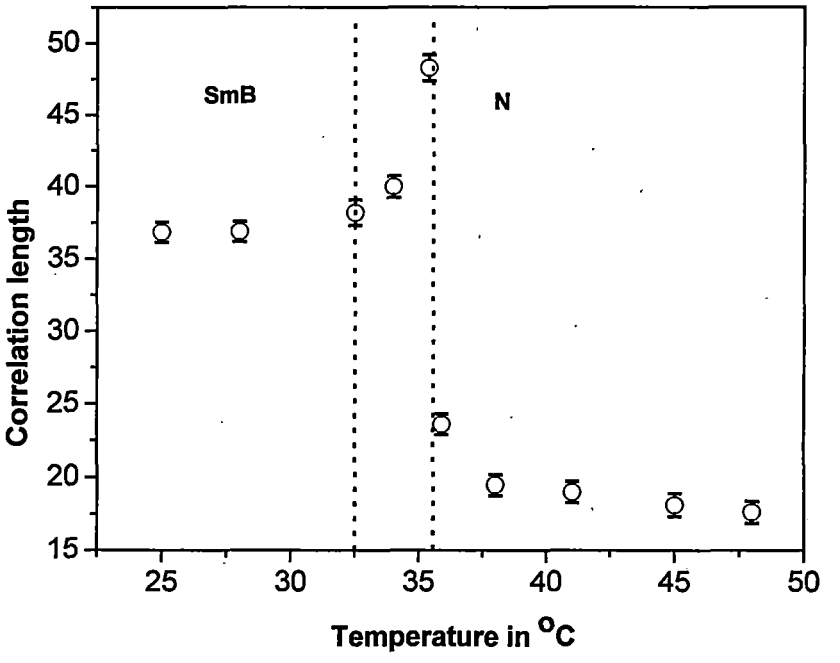

FIGURE 7.12: Temperature variation of transverse correlation length of mixture A.

Figure 7.12 shows the measurements of transverse correlation length over the entire mesomorphic temperature region for mixture A. These values are found to diverge as the co-existing phase region is approached from either side, indicating a second order phase transition. This has been supported by entropy, density, refractive index and OOP measurements. The temperature variation of transverse correlation length for mixture B also shows a similar trend.

The angular distribution of the x-ray diffraction intensities for mixtures A and B are used to measure the orientational distribution function $f(\theta)$ and hence the orientational order parameter $\langle P_2 \rangle$ and $\langle P_4 \rangle$ throughout their entire mesomorphic range following a procedure described in chapter 2.

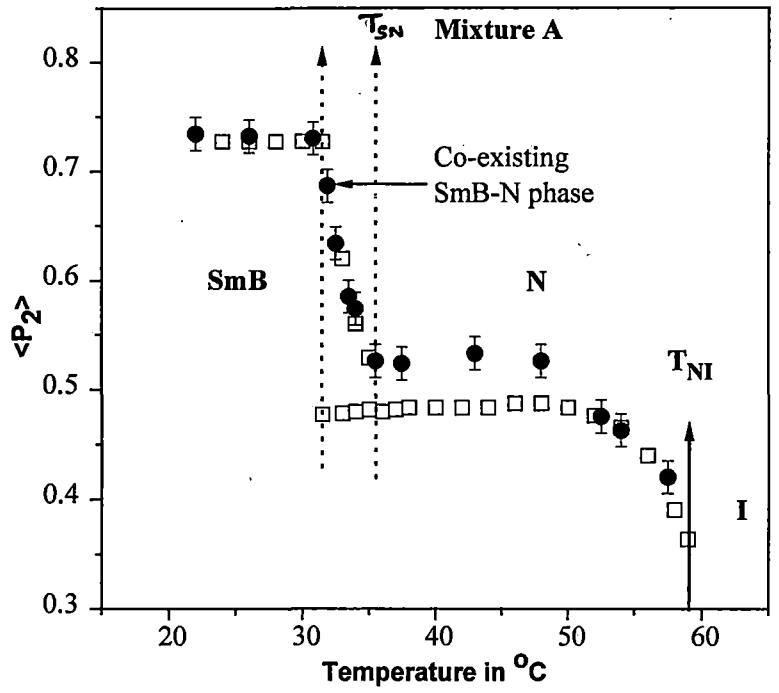

FIGURE 7.13: Temperature dependences of <P_2> values for mixture A. □ <P_2> from refractive index data, ● <P_2> from x-ray data. T_{NI} = nematic – isotropic transition temperature. T_{SN} = smectic B – nematic transition temperature.

Figures 7.13 and 7.14 show the variation of the experimentally determined OOP's with temperature for the two mixtures A and B respectively. The experimental <P_2> and <P_4> values are relatively high in the smectic B phase, showing the phase to be much more orientationally ordered than its neighbouring nematic phase. In the coexisting SmB-N phase a very sharp decrease of the OOP values is observed with increase in temperature. This OOP is in effect the weighted mean OOP of the two phases. This is due to the fact that in this two-phase region, the SmB domains rapidly reduce in size with increasing temperature, so that the weighted mean OOP decreases rather rapidly. Similar results are also observed in the OOP values obtained

from the refractive index measurements, which are also indicated in the respective figures.

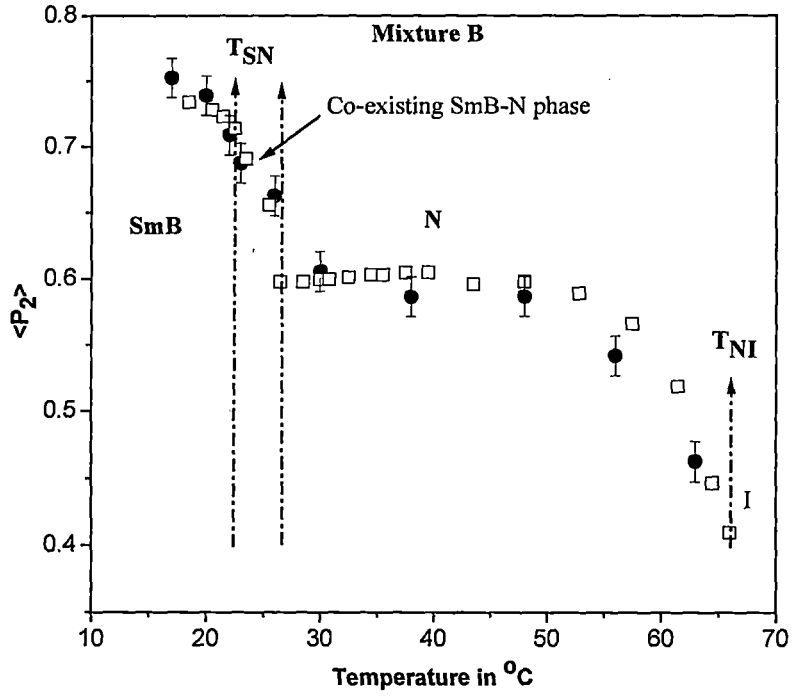

FIGURE 7.14: Temperature dependences of $<P_2>$ values for mixture B. □ $<P_2>$ from refractive index data, ● $<P_2>$ from x-ray data. T_{NI} = nematic – isotropic transition temperature. T_{SN} = smectic B – nematic transition temperature.

The values of the apparent molecular length or layer thickness (d) and the intermolecular distance (D), at different temperatures are also measured for mixtures with x = 0.3, 0.4, 0.5, 0.6, 0.73. The temperature variation of the intermolecular distance, D, for mixtures A and B throughout the mesomorphic range are shown in figure 7.15. There is an increase in the D values from the Smectic B to nematic phase transition. This increase is most sharp at the transition to the co-existing phase and these values also continue to increase within this phase. The reason for this is the same as stated for the variation of OOP in the two-phase region. As observed from figure 7.15, the

variation of D with temperature in the nematic phase is quite appreciable, caused due to the increasing thermal vibrations of the chain parts of these flexible molecules.

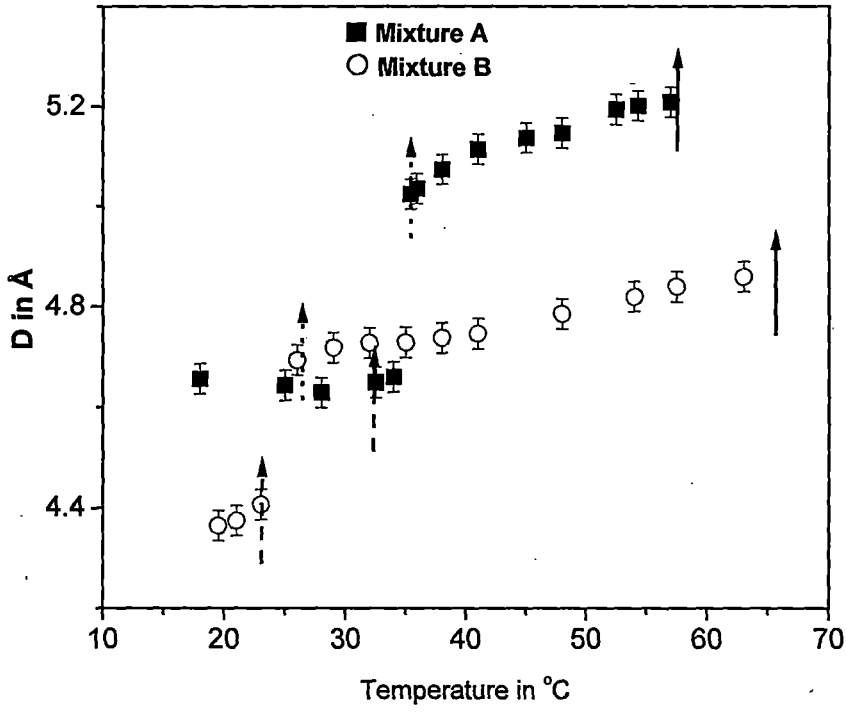

FIGURE 7.15: Temperature dependences of D values for mixtures A and B. Key to symbols: ■ Mixture A ○ Mixture B

As expected, the temperature variation of d in the smectic phase is slight. However, for all the mixtures the apparent molecular lengths (l) increases with increasing temperature and the effect is pronounced near the nematic-isotropic phase transition (figure 7.16). This increase before the phase transition is once again due to the increasing thermal vibrations of their chain parts just before the transition.

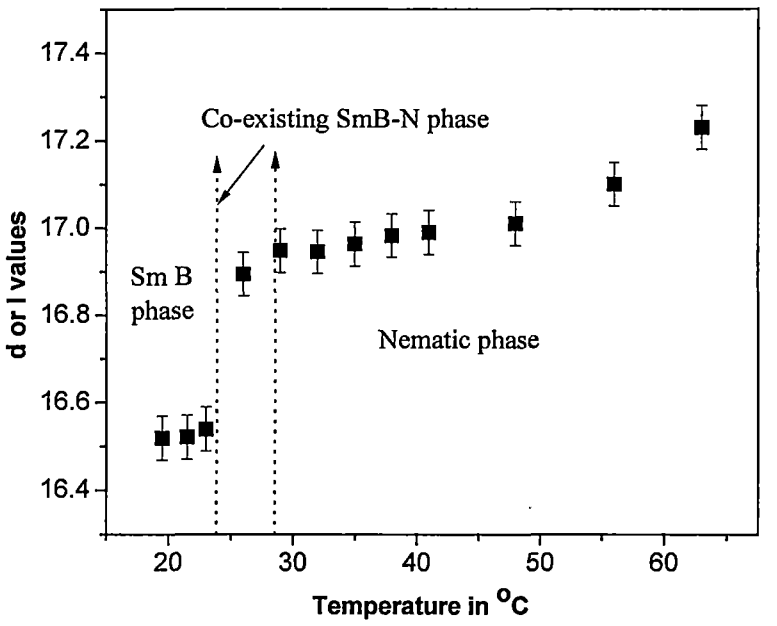

FIGURE 7.16: Temperature variations of apparent molecular length (l) or layer thickness (d) values.

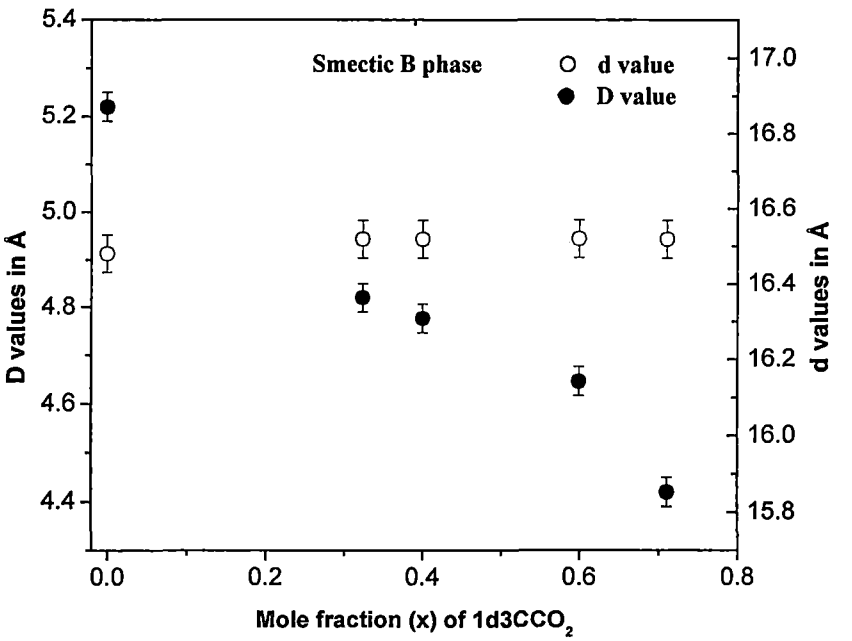

FIGURE 7.17: Variations of D (●) and d (○) values with mole fraction (x) in smectic B phase.

The d values in the smectic B phase are more or less the same for all the mixtures (figure 7.17) and are almost equal to the respective model molecular lengths of the isomeric pure components. However, the D values in the smectic B phase decreases with the increase in mole fraction of 1d(3)CCO_2 . At a temperature T = T_{NI}-2.5°C, in the nematic phase of this system, the D values show an enhancement in their magnitudes near x≈0.6 (figure 7.18), whereas the density and order parameter show a reverse trend. This implies that the packing of the molecules in nematic phase is rather poor near this region. The l values in the nematic phase however, slightly increases with increase in the mole fraction of 1d(3)CCO_2.

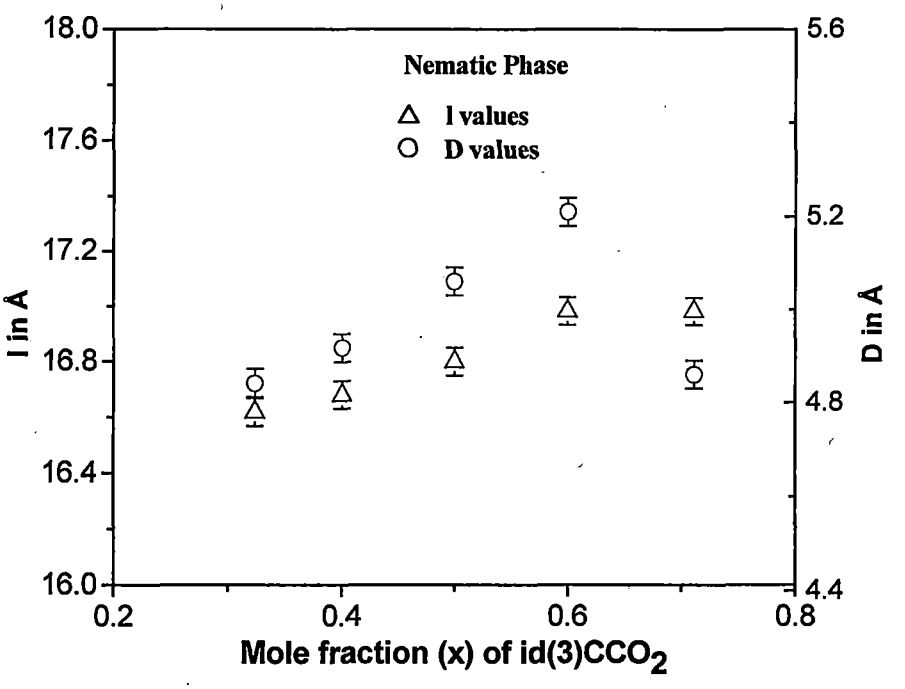

FIGURE 7.18: Variations of l (△) and D (○) values with mole fraction (x) in nematic phase.

REFERENCES:

[1] A. Nath, B. Chaudhury and S. Paul, *Mol. Cryst. Liq. Cryst.* **265**, 699 (1995).

[2] B. Adhikari and R. Paul, *Phase transitions*, **56**, 165 (1996).

[3] A. Nath, S. Gupta, P. Mandal, S. Paul and H. Schenk, *Liq. Cryst.*, **20**, 765 (1996).

[4] A. Nath, Chaudhury, B. Paul and S. Paul, *Mol. Cryst. Liq. Cryst.*, **265A**, 699 (1995).

[5] M. Schad, R. Buchecker and K. Müller, *Liq. Cryst.*, **5**, 293 (1989).

[6] R. J. Birgeneau and J. D. Lister, *J. Phys. Lett.*, **39**, L-399 (1978).

[7] C. C. Haung and T. Stoebe, *Adv. Phys.*, **42**, 343 (1993).

[8] G. J. Brownsey, & A. J. Leadbetter, *Phys. Rev. Lett.* **44**, 1608 (1980).

[9] P. A. C. Gane and A. J. Leadbetter, *J. Phys. C.: Solid State Phys.*, **16**, 2059 (1983).

[10] C. V. Lobo, S. Krishna Prasad and D. S. Shankar Rao, *Phy. Rev. E*, **69**, 051706 (2004).

[11] D. E. Moncton and R. Pindak, *Phy. Rev. Lett.*, **43**, 701 (1979).

[12] C. C. Haung and K. J. Strandburg, (Ed.), *"Bond Orientational Order in Condensed Matter Systems"*, Springer-Verlag, Berlin, pp 78 (1992).

[13] J. Doucet, A. M. Levelut and M. Lambert, *Ann. Phys.*, **3**, 157 (1978).

[14] A. J. Kim, M. Veum, T. Stoebe, C. F. Chou, , J. T. Ho, , S. W. Hui, , V. Surendranath and C. C. Haung, *Phy. Rev. Letts.*, **74**, no24, 4863 (1995).

[15] M. Cheng, J. H. Ho, S. W. Hui and R. Pindak, *Phys. Rev. Letts.*, **59**, 1112 (1987).

[16] A. K. Zeminder, S. Paul, and R. Paul, *Mol. Cryst. Liq. Cryst.*, **61**, 191 (1980).

[17] H. E. J. Neugabauer, *Can. J. Phys.*, **32**, 1 (1954).

[18] I. Haller, H. A. Huggins, H. R. Lilienthal and T. R. McGuire, *J. Phys. Chem.* **77**, 900 (1973).

[19] H. P. Klug and L. E. Alexander, *"X-ray diffraction procedure for polycrystalline and amorphous materials"*, John Wiley and Sons, New York, page 114 and 473 (1974).

[20] B. K. Vainshtein, *"Diffraction of x-rays by chain molecules"*, Elsevier Pub. Co., London (1966).